Dual electronic states in thermoelectric cobalt oxide [Bi 1.7 Ca 2 O 4] 0.59 CoO 2

Patrice Limelette, Sylvie Hebert, Hervé Muguerra, Raymond Frésard, Charles Simon

Dual electronic states in thermoelectric cobalt oxide $[Bi_{1.7}Ca_2O_4]_{0.59}CoO_2$

Patrice Limelette,[1] Sylvie Hébert,[2] Hervé Muguerra,[2] Raymond Frésard,[2] and Charles Simon[2]
[1]*Laboratoire LEMA, UMR 6157 CNRS-CEA, Université F. Rabelais, UFR Sciences, Parc de Grandmont, 37200 Tours Cedex, France*
[2]*Laboratoire CRISMAT, UMR CNRS–ENSICAEN (ISMRA) 6508, 6, Boulevard du Maréchal Juin, 14050 CAEN Cedex, France*
(Received 4 October 2007; revised manuscript received 21 March 2008; published 25 June 2008)

We investigate the low-temperature magnetic-field dependence of the resistivity in the thermoelectric misfit cobalt oxide $[Bi_{1.7}Ca_2O_4]_{0.59}CoO_2$ from 60 K down to 3 K. The scaling of the negative magnetoresistance demonstrates a spin dependent transport mechanism due to a strong Hund's coupling. The inferred microscopic description implies dual electronic states, which explain the coexistence between localized and itinerant electrons both contributing to the thermopower. By shedding light on the electronic states, which lead to a high thermopower, this result likely provides potential way to optimize the thermoelectric properties.

DOI: 10.1103/PhysRevB.77.235118 PACS number(s): 72.15.Jf, 71.27.+a, 72.25.−b

I. INTRODUCTION

By converting heat into voltage, thermoelectric materials are not only of major interest in both energy saving and cooling applications but they also bring a fundamental challenge in order to find the physical limits optimizing their performance. As stated by Mahan and Sofo,[1] this problem can be formulated as follows: *What is the best electronic structure a thermoelectric can have?* In their answer they stress that the energy distribution of the charge carriers should be as narrow as possible,[1] thus emphasizing the relevance of correlated materials to thermoelectricity as those in the vicinity of a Mott metal-insulator transition.[2–4] In particular, layered cobaltates seem to belong to this class of materials:[5] they exhibit interesting properties,[6] including superconductivity[7] and both metallicklike resistivity and large thermopower at room temperature. In particular, it has been recently pointed out that their large thermopower could both result from extended quasiparticles with an enhanced effective mass and from an entropy contribution of localized spins.[8] Indeed the room-temperature thermopower is large in the whole series of cobalt misfits and does not depend on the nature of the separating layers.[9] In misfits, it ranges from 75 μV/K in $[Sr_2O_{2-\delta}]_{0.53}[CoO_2]$ as observed by Ishiwata *et al.*,[10] to 350 μV/K in $(CaOH)_{1.14}CoO_2$ (Ref. 11), the former value being close to the expected value for an assembly of free spin 1/2. On the other hand, a lack of systematic trend has been shown for both resistivity and thermopower of these systems at low temperature.[9] The low-temperature thermopower exhibits a strong magnetic-field dependence in BiCaCoO and in Na_xCoO_2 (Ref. 12) but not in BiBaCoO (Ref. 13). While for most cobaltates, there is a large temperature range where the thermopower is T linear. This behavior does not extrapolate to zero at zero temperature in BiCaCoO, in contrast to, e.g., BiBaCoO (Ref. 14). Furthermore, it is known that the entropic contribution[12,14–16] or the electronic correlations[2,3,5,17–19] can increase thermopower. These two additive contributions further raise the aforementioned issue: what is the nature of the electronic states relevant to the transport?

To that aim, we report in this paper the crossed experimental investigation of the magnetoresistance and thermopower in single-crystal cobalt oxide $[Bi_{1.7}Ca_2O_4]_{0.59}CoO_2$, here used as a probe aimed at characterizing the coupling between itinerant and localized states. While a large negative magnetoresistance was already measured in sintered samples,[14] we demonstrate here that it follows a scaling behavior with both magnetic field and temperature. Originally introduced in the context of the colossal magnetoresistance of the manganites,[20,21] this scaling implies a spin dependent transport mechanism. Thus, we show that the analysis of the negative magnetoresistance allows us to shed light on the electronic states leading to high thermopower.

Similarly to Na_xCoO_2, the structure of the incommensurate cobalt oxide $[Bi_{1.7}Ca_2O_4]_{0.59}CoO_2$ (abbreviated thereafter BiCaCoO) contains single $[CoO_2]$ layer of CdI_2 type stacked with rocksalt-type layers instead of a sodium deficient layer as displayed in Fig. 1. One of the in-plane sublattice parameters being different from one layer to the

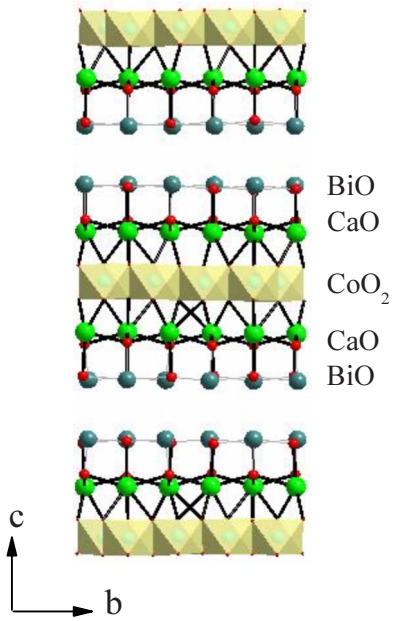

FIG. 1. (Color online). Schematic picture of the crystal structure of the cobaltate $[Bi_{1.7}Ca_2O_4]_{0.59}CoO_2$.

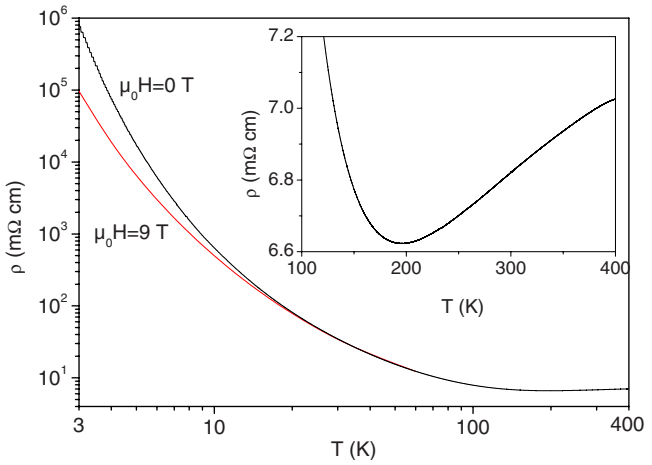

FIG. 2. (Color online). Temperature dependences of the single-crystal in-plane resistivity ρ at 0 and 9 T, the magnetic field being parallel to the conducting plane. The inset displays a transport crossover from a high-temperature metalliclike behavior to a low-temperature insulatinglike one.

other,[14,22] the cobaltate BiCaCoO has a misfit structure as in most related compounds.[14,22,23] This system exhibits, at room temperature, a very large holelike thermopower $S \approx 138\ \mu VK^{-1}$ and a rather low resistivity as in the so-called *bad* metals near a Mott metal-insulator transition.[4,14,24]

II. TRANSPORT MEASUREMENTS

In order to investigate the transport properties and more specifically the magnetoresistance in BiCaCoO, we have measured the single-crystal in-plane resistivity $\rho(H,T)$ using a standard four terminal method. The studied single crystals were grown using a standard flux method,[22] with typical sizes of the order of $4\times2\times0.02\ mm^3$. As displayed in the inset of Fig. 2, the temperature dependence of the resistivity exhibits a transport crossover around 200 K from a high-temperature metalliclike behavior to a low-temperature insulatinglike one. While in the former regime the values of the resistivity remain rather low, Fig. 2 displays a large enhancement of ρ at low temperature indicating thus an efficient localization process. Remarkably the latter is strongly suppressed by the application of an in-plane magnetic field with a reduction in 85 % at 9 T at the lowest temperature, which is in marked contrast with the conventional Anderson localization scenario.

A. Magnetoresistance

In order to gain a better insight into this state, we have performed transport measurements as a function of an in-plane magnetic field H at constant temperature T. The data reported in the inset of Fig. 3 spans the T range from 60 K down to 3 K where the magnetoresistance is large and negative. Also, Fig. 3 demonstrates that the whole set of magnetoresistance data can be scaled onto a variable range hopping form (abbreviated thereafter VRH), which can be written as follows:

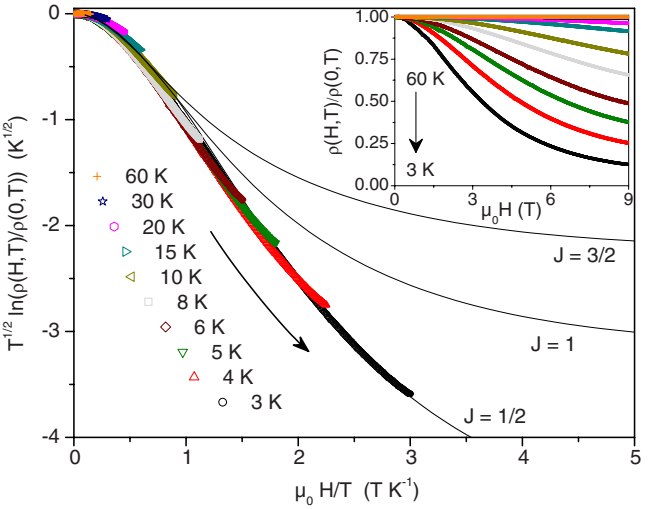

FIG. 3. (Color online). Scaling plot of the single-crystal in-plane resistivity $\rho(H,T)$ as a function of $\mu_0 H/T$. The inset displays the magnetic-field dependence of the normalized resistivity over the whole temperature range. The applied magnetic field is parallel to the conducting plane.

$$\rho(H,T) = \rho_0(T)\exp\left[\frac{\tau_0(H/T)}{T}\right]^{\alpha}. \quad (1)$$

While the two exponents $\alpha=1/2$ and 1/3 lead to satisfactory scalings, it is worth noting that the value $\alpha=1/2$ provides the best collapse of the experimental points onto a single curve. Originally introduced by Mott[25] to describe the electronic conduction in disordered materials, the VRH theory essentially leads to the exponents $\alpha=1/4$ or 1/3 in three or two dimensions, and $\alpha=1/2$ in disordered systems with electron correlations.

More recently, the VRH mechanism has been extended to the case of magnetic disorder to explain the colossal negative magnetoresistance measured in manganites[20,21] and also applied in the Chromium based spinel compounds.[26] The main ideas, which underlie this conducting process, are consist in a variable range spin dependent hopping (VRSDH) due to the Hund's coupling $-J_H\mathbf{s}.\ \sigma$ between the quasiparticles spin s and the localized spin σ, with the Hund's coupling constant J_H. To basically illustrate this mechanism, let us consider the propagation of a quasiparticle with a spin s_i from site i to site j as sketched in Fig. 4 with the involved spin polarized electronic energy levels.

By assuming a paramagnetic state, namely localized spins uncorrelated from one site to another, there is a probability to find an angle θ_{ij} between σ_i and the neighbor localized spin σ_j. Because s_i points along the localized spin σ_i direction, the aforementioned misorientation leads to a magnetic potential barrier $\Delta_{ij}=\Delta\ (1-\cos\theta_{ij})/2$ with $\Delta=2J_H\ s\sigma$. At this very qualitative stage one can infer two important consequences, which both agree with the experimental results reported in Fig. 3. First, the magnetic potential barriers are randomly distributed in such a paramagnetic material, namely, there is a magnetic disorder that implies VRH conduction. Besides, an applied magnetic field tends to align the localized spins and thus lowers both Δ_{ij} and the disorder, suggesting a negative magnetoresistance.

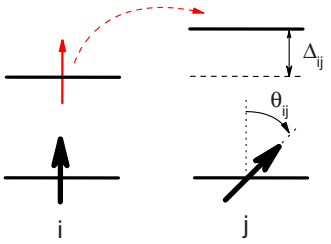

FIG. 4. (Color online). Schematic picture of the electronic energy levels involved in an elementary spin dependent hopping from site i to site j. The magnetic potential barrier Δ_{ij} results from the misorientation θ_{ij} between the quasiparticle spin s_i (thin red arrow) and the localized spin σ_j (bold black arrow) as explained in the text.

In order to give a deeper insight into the spin dependent hopping that is more extensively developed in Ref. 20, an analogy can be performed with the conventional VRH process. In the latter case, the resistivity varies as $\rho \propto \exp(T_0/T)^{\alpha}$ with $T_0 \propto 1/[\xi^3 g(E_F)]$, ξ being the localization length, and $g(E_F)$ the density of states (DOS) at the Fermi level.[25] Without any magnetic field, the VRSDH resistivity should thus depend on a parameter $\tau_0 \propto 1/[\xi^3 n(\Delta_{ij})]$ as in Eq. (1), with $n(\Delta_{ij})$ the DOS of the magnetic potential barriers.

Within this framework, the latter DOS can then be deduced from the probability of finding an angle θ_{ij} as $n(\Delta_{ij}) \approx 1/\Delta$. Also, this constant DOS implies an average magnetic potential barrier $\langle \Delta_{ij} \rangle = \Delta/2$. The latter mean value is no longer valid when a magnetic field is applied because $\langle \cos \theta_{ij} \rangle \neq 0$, and it must be written as $\langle \Delta_{ij} \rangle = \Delta(1 - \langle \cos \theta_{ij} \rangle)/2$. In this case, the misorientation can be expressed from the local magnetizations $\vec{M}_{i,j}$ at the two sites i and j as $\langle \vec{M}_i \cdot \vec{M}_j \rangle = M_S^2 \langle \cos \theta_{ij} \rangle$, with the saturation magnetization M_S. Since there are no short-range correlations in a paramagnet, the averaged magnetization is supposed to scale as the Brillouin function $B_J(x)$ as discussed by Wagner *et al.*[21] It is given by

$$B_J(x) = \frac{2J+1}{2J}\coth[(2J+1)x] - \frac{1}{2J}\coth(x). \qquad (2)$$

Here J is the angular momentum, $x = (g\mu_B H)/(2k_B T)$, $g=2$ is the Landé factor, k_B is the Boltzmann constant, and μ_B is the Bohr magneton.

As a consequence, one deduces that $\langle \cos \theta_{ij} \rangle = B_J(x)^2$ and thus the averaged magnetic potential barrier is $\langle \Delta_{ij} \rangle = \Delta\,[1 - B_J(x)^2]/2$. Since it is lowered from its value without magnetic field by the factor $[1 - B_J(x)^2]$, one may infer that the DOS is enhanced as $n(\Delta_{ij}) \approx 1/\{\Delta[1 - B_J(x)^2]\}$ by assuming that it keeps constant over the whole range of potential. In this approximation, the temperature $\tau_0(x)$ can be written following Eq. (3) with the unit-cell volume v.

$$\tau_0(x) = [1 - B_J(x)^2]T_0^M \quad \text{and} \quad T_0^M \approx \frac{v}{\xi^3}\frac{\Delta}{k_B}. \qquad (3)$$

The combination of both Eqs. (1) and (3) leads to a complete analytic expression of the magnetoresistance with the only two parameters J and T_0^M that yields to the curves in Fig. 3 compared to the experimental data. The three tested

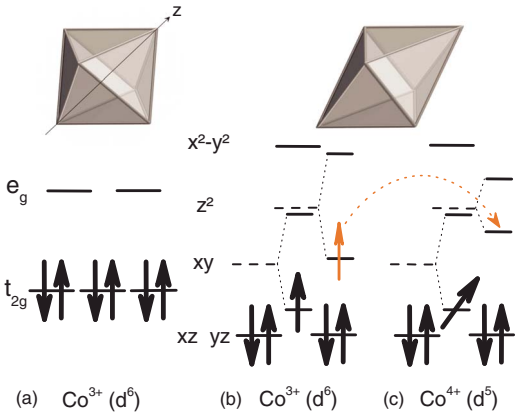

FIG. 5. (Color online). (a): Crystal-field effect in the Co^{3+} (d^6). (b): The structural distortion along the z axis illustrated by the two upper octahedrons reduces the gap between the d_{z^2} and the d_{xy} levels. A strong Hund's coupling is, besides, represented with the splitting of the two spin states in the d_{z^2} and d_{xy} levels, respectively. (b) and (c): Spin dependent hopping mechanism between the Co^{3+} and the Co^{4+}. The thin red arrow represents the quasiparticle spin and the bold black arrows the localized spin.

sets of parameters with $J=1/2$ ($T_0^M = 24$ K), $J=1$ ($T_0^M = 12$ K), and $J=3/2$ ($T_0^M = 6$ K) demonstrate unambiguously the agreement with $J=1/2$ by also confirming the relevance of the analysis. One can here emphasize that the found rather low value of T_0^M is consistent with a VRH transport since it suggests as required a localization length exceeding the interatomic distances. Beyond these strong checks, this result implies that the localized spin involved here in the VRSDH mechanism in BiCaCoO is $\sigma=1/2$ as previously inferred from the analysis of the magnetic-field dependence of the thermopower[8] and in agreement with the previously reported susceptibility measurements.[14] As a consequence, it seems that both extended and localized states not only coexist but also give rise to unusual electronic properties as large negative magnetoresistance and high thermopower.

Let us now discuss the relevance of the electronic levels as sketched in Fig. 4 in BiCaCoO. By analogy with the crystallographic structure of Na_xCoO_2 (Ref. 27), the $[CoO_2]$ planes in the misfit cobaltates are assumed to be conducting and are stacked with the insulating rocksalt-type layers. These $[CoO_2]$ layers consist in a 2D triangular lattice Co sheets octahedrally coordinated with O above and below the Co plane. As depicted in Fig. 5, the Co d levels are first crystal-field split in the octahedral O environment into a lower-lying t_{2g} and an upper-lying e_g manifold. In this context, the six electrons of the Co^{3+} (d^6) occupy the t_{2g} levels [see Fig. 5(a)]. Second, the difference in energy between the d_{z^2} and d_{xy} levels can be reduced assuming a structural distortion of the octahedron following from stretching of the z axis. Therefore, for sufficiently strong Hund's coupling, the gap between the d_{z^2} and the d_{xy} levels can become smaller than the Hund's rule splitting, i.e., the spin-up d_{z^2} energy can get smaller than the spin-down d_{xy} energy. As a result, the scattering of itinerant e_g electrons hopping from site to site by the localized t_{2g} electrons, as illustrated in Figs. 5(b) and 5(c), leads to the same electronic background as in Fig. 4,

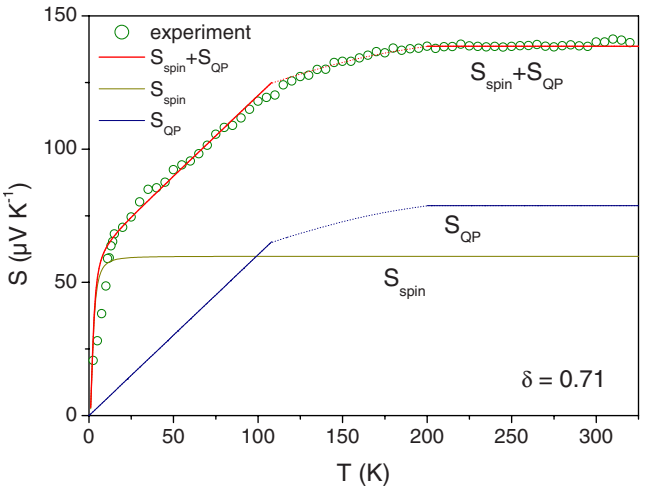

FIG. 6. (Color online). Comparison between the experimental temperature dependence of the thermopower S (Ref. 14) and the theoretical predictions including both localized spins S_{spin} and quasiparticles S_{QP} contributions. It is worth noting that the latter is plotted from the two limiting cases, namely, with $S_{\mathrm{QP}} \approx \pi^2/6, k_B/e$, and T/T_F^* if $T \ll T_F^*$ and $S_{\mathrm{QP}} = k_B/e \ln[\delta/(1-\delta)]$ if $T > T_F^*$.

and explains the above-mentioned negative magnetoresistance.

Even if this situation can be achieved from other scenarios, possibly involving the a_{1g} and e_g' orbitals due to the triangular lattice, we emphasize that the aforementioned ingredients must remain to explain the magnetoresistance, namely, a distortion and a Hund's splitting, which reduce the $t_{2g}-e_g$ gap and spin polarize the electronic levels. Also, it is worth noting that a similar description with a strong coupling between the spin and the orbital degrees of freedom has been quite recently proposed in order to explain the magnetic properties in the parent compound Na_xCoO_2 (Ref. 28).

B. Thermopower

We now would like to address more specifically the connection between the electronic levels represented in Figs. 5(b) and 5(c) and the thermopower S measured in BiCaCoO and reported in Fig. 6 (Ref. 8).

According to Figs. 5(b) and 5(c), the t_{2g} electrons are localized ($\sigma = 1/2$), while the lower e_g electron ($s = 1/2$) are itinerant, preventing them from forming local triplet states on long time scales. Since the localized spins σ remain paramagnetic, they asymptotically give rise to a thermopower contribution $S_{\mathrm{spin}} = k_B/e \ln(2)$ due to their spin entropy as displayed in Fig. 6, with e as the elementary electric charge. In order to provide a constant contribution over a wide temperature range, it is here assumed that their energy level is located in an energy width of a few tens of Kelvin below the Fermi level and that it does not hybridize with the e_g band. We stress that the latter interpretation is consistent with the fact that these spins are also responsible for a negative magnetothermopower.[8]

On the other hand, the e_g quasiparticles are expected to contribute to the thermopower as $S_{\mathrm{QP}} \propto T/T_F^*$ at temperatures lower than the effective Fermi temperature $T_F^* \approx T_F/m^*$. Here T_F is the bare Fermi temperature and m^* is the effective mass, which takes into account the electronic correlations.[2,3] Note that, according to Pálsson and Kotliar,[2] the thermopower does not depend on the scattering rate in the low-temperature regime. Also, a rough estimate of the effective Fermi temperature inferred from the slope of S leads to a very low value ($230K < T_F^* < 260K$), which implies an enhanced m^* in agreement with the observed constant thermopower for $T > T_F^*$. In fact, at temperatures higher than T_F^* the e_g electronic excitations become incoherent and the related thermopower recovers a purely entropic form following Eq. (4). In this regime, the thermopower is temperature independent and reads,

$$S_{\mathrm{QP}}(T > T_F^*) = \frac{k_B}{e} \ln\left[\frac{\delta}{N(1-\delta)}\right], \tag{4}$$

with the degeneracy N involving both spin and orbital degrees of freedom[2] and the electronic filling factor δ. Moreover, because of their spin polarized level the e_g electrons have no more spin degeneracy, implying, thus, $N=1$ in Eq. (4). By adding the two aforementioned entropic contributions in Fig. 6, namely, those originating from both the paramagnetic spins (the t_{2g} electrons) and the quasiparticles (the e_g electrons), one can therefore deduce the filling factor $\delta \approx 0.71$ corresponding to 0.29 hole. Let us finally discuss the electronic properties of the parent compound BiBaCoO (Ref. 13). This cobaltate exhibits neither negative magnetoresistance nor negative magnetothermopower. The low-temperature linear in T dependence of S extrapolates to zero in contrast to Fig. 6, suggesting that only extended states contribute to the thermopower in this compound. Also, the room-temperature value of the thermopower is of the order of 90 $\mu\mathrm{VK}^{-1}$, namely, 50 $\mu\mathrm{VK}^{-1}$ less than in BiCaCoO. As a strong check of the whole reported analysis, this comparison clearly demonstrates, by invalidating the presence of localized paramagnetic spins in BiBaCoO, that these dual electronic states are a source of an enhanced thermopower. Further experimental investigations are now needed in order to understand why these coexisting states are not observed in BiBaCoO in contrast to BiCaCoO.

III. CONCLUSION

To conclude, we have investigated the low-temperature magnetic-field dependence of the resistivity in the thermoelectric misfit cobalt oxide BiCaCoO from 60 K down to 3 K. The scaling of the negative magnetoresistance demonstrates a spin dependent transport mechanism due to a strong Hund's coupling. The inferred microscopic description implies dual electronic states, which explain the coexistence between localized and itinerant electrons both contributing to the thermopower. By shedding light on the electronic states leading to a high thermopower, this result likely provides a potential way to optimize the thermoelectric properties.

ACKNOWLEDGMENTS

We are grateful to F. Ladieu and D. Grebille for the illuminating discussions.

[1] G. Mahan and J. Sofo, Proc. Natl. Acad. Sci. U.S.A. **93**, 7436 (1996); G. Mahan, B. Sales, and J. Sharp, Phys. Today **50** (3), 42 (1997).
[2] G. Pálsson and G. Kotliar, Phys. Rev. Lett. **80**, 4775 (1998).
[3] J. Merino and R. H. McKenzie, Phys. Rev. B **61**, 7996 (2000).
[4] A. Georges, G. Kotliar, W. Krauth, and M. J. Rozenberg, Rev. Mod. Phys. **68**, 13 (1996).
[5] P. Limelette, V. Hardy, P. Auban-Senzier, D. Jérome, D. Flahaut, S. Hébert, R. Frésard, C. Simon, J. Noudem, and A. Maignan, Phys. Rev. B **71**, 233108 (2005).
[6] I. Terasaki, Y. Sasago, and K. Uchinokura, Phys. Rev. B **56**, R12685 (1997).
[7] K. Takada, H. Sakurai, E. Takayama-Muromachi, F. Izumi, R. Dilanian, and T. Sasaki, Nature (London) **422**, 53 (2003).
[8] P. Limelette, S. Hébert, V. Hardy, R. Frésard, C. Simon, and A. Maignan, Phys. Rev. Lett. **97**, 046601 (2006).
[9] J. Bobroff, S. Hébert, G. Lang, P. Mendels, D. Pelloquin, and A. Maignan, Phys. Rev. B **76**, 100407(R) (2007).
[10] S. Ishiwata, I. Terasaki, Y. Kusano, and M. Takano, J. Phys. Soc. Jpn. **75**, 104716 (2006).
[11] M. Shizuya, M. Isobe, Y. Baba, T. Nagai, M. Osada, K. Kosuda, S. Takenouchi, Y. Matsui, and E. Takayama- Muromachi, J. Solid State Chem. **180**, 249 (2007).
[12] Y. Wang, N. Rogado, R. Cava, and N. Ong, Nature (London) **423**, 425 (2003).
[13] M. Hervieu, A. Maignan, C. Michel, V. Hardy, N. Créon, and B. Raveau, Phys. Rev. B **67**, 045112 (2003).
[14] A. Maignan, S. Hébert, M. Hervieu, C. Michel, D. Pelloquin, and D. Khomskii, J. Phys.: Condens. Matter **15**, 2711 (2003).
[15] W. Koshibae, K. Tsutsui, and S. Maekawa, Phys. Rev. B **62**, 6869 (2000).
[16] K. Koumoto, I. Terasaki, and M. Murayama, *Oxide Thermoelectrics* (Research Signpost, India, 2002).
[17] K. Behnia, D. Jaccard, and J. Flouquet, J. Phys.: Condens. Matter **16**, 5187 (2004).
[18] O. I. Motrunich and P. A. Lee, Phys. Rev. B **69**, 214516 (2004).
[19] R. Frésard, Ch. Martin, S. Hébert, A. Maignan, L. Pi, B. Raveau, and J. Hejtmanek, Phys. Lett. A **303**, 223 (2002).
[20] M. Viret, L. Ranno, and J. M. D. Coey, Phys. Rev. B **55**, 8067 (1997).
[21] P. Wagner, I. Gordon, L. Trappeniers, J. Vanacken, F. Herlach, V. V. Moshchalkov, and Y. Bruynseraede, Phys. Rev. Lett. **81**, 3980 (1998).
[22] H. Leligny, D. Grebille, O. P. A. Masset, M. Hervieu, C. Michel, and B. Raveau, C.R. Acad. Sci., Ser. IIc: Chim **2**, 409 (1999).
[23] D. Grebille, H. Muguerra, O. Pérez, E. Guilmeau, H. Rousselière, and R. Funahashi, Acta Crystallogr., Sect. B: Struct. Sci. **63**, 373 (2007).
[24] P. Limelette, P. Wzietek, S. Florens, A. Georges, T. A. Costi, C. Pasquier, D. Jérome, C. Méziére, and P. Batail, Phys. Rev. Lett. **91**, 016401 (2003).
[25] N. F. Mott and E. A. Davis *Electronic Processes in Non Crystalline Materials* (Clarendon, Oxford, 1979); A. L. Efros and B. L. Shklovskii, J. Phys. C **8**, L49 (1975).
[26] M. Muroi, R. Street, and P. G. McCormick, Phys. Rev. B **63**, 052412 (2001).
[27] D. J. Singh, Phys. Rev. B **61**, 13397 (2000).
[28] M. Daghofer, P. Horsch, and G. Khaliullin, Phys. Rev. Lett. **96**, 216404 (2006).